Atmospheric
Chemistry
and Physics

Open Access

Variability in the speed of the Brewer–Dobson circulation as observed by Aura/MLS

T. Flury[1,*], D. L. Wu[2], and W. G. Read[1]

[1]Jet Propulsion Laboratory, California Institute of Technology, Pasadena, California, USA
[2]NASA-Goddard Space Flight Center, Greenbelt, Maryland, USA
[*]now at: Swiss Federal Office of Public Health, Bern, Switzerland

*Correspondence to:* T. Flury (thomas.flury@yahoo.com)

Abstract. We use Aura/MLS stratospheric water vapour (H_2O) measurements as tracer for dynamics and infer inter-annual variations in the speed of the Brewer–Dobson circulation (BDC) from 2004 to 2011. We correlate one-year time series of H_2O in the lower stratosphere at two subsequent pressure levels (68 hPa, ∼18.8 km and 56 hPa, ∼19.9 km at the Equator) and determine the time lag for best correlation. The same calculation is made on the horizontal on the 100 hPa (∼16.6 km) level by correlating the H_2O time series at the Equator with the ones at 40° N and 40° S. From these lag coefficients we derive the vertical and horizontal speeds of the BDC in the tropics and extra-tropics, respectively. We observe a clear interannual variability of the vertical and horizontal branch. The variability reflects signatures of the Quasi Biennial Oscillation (QBO). Our measurements confirm the QBO meridional circulation anomalies and show that the speed variations in the two branches of the BDC are out of phase and fairly well anti-correlated. Maximum ascent rates are found during the QBO easterly phase. We also find that transport of H_2O towards the Northern Hemisphere (NH) is on the average two times faster than to the Southern Hemisphere (SH) with a mean speed of 1.15 m s^{-1} at 100 hPa. Furthermore, the speed towards the NH shows much more interannual variability with an amplitude of about 21 % whilst the speed towards the SH varies by only 10 %. An amplitude of 21 % is also observed in the variability of the ascent rate at the Equator which is on the average 0.2 mm s^{-1}.

1 Introduction

The very low amounts of water vapour (H_2O) measured in the lower stratosphere by Brewer (1949) implied that air masses must be entering the stratosphere through the cold tropical tropopause because nowhere else temperatures are low enough to allow for sufficient dehydration. Dobson (1956) used ground-based measurements of total ozone and observed minimum values in the photo-chemical source region of the tropics and maximum values in the extra-tropics. Hence, he assumed a transport from the tropical stratosphere towards the pole in both hemispheres marked by low-latitude ascent and high-latitude descent. The assumption of a pole-ward residual circulation now called Brewer–Dobson circulation (BDC) is still valid today. Figure 1 shows the different branches of the BDC (adapted from Plumb, 2002). Air masses ascend inside the tropical pipe, which represents a mixing barrier for tropical and extra-tropical air (Plumb, 1996). The rising air is distributed symmetrically towards both hemispheres in the lowermost stratosphere (black arrows) and brings H_2O from low- to high-latitudes. The lower stratospheric meridional component is usually called shallow branch of the BDC and is faster during summer (Bönisch et al., 2009) when air masses are quasi horizontally mixed out of the tropics. Mixing into the tropics is slow compared to mixing within mid-latitudes (Volk et al., 1996) highlighted by a smaller arrow pointing back towards the Equator. In the upper stratosphere air masses are predominantly directed towards the winter pole where they mix and descend into the so called "surf zone" and the polar vortex. This is called the deep branch of the BDC which is relatively slow
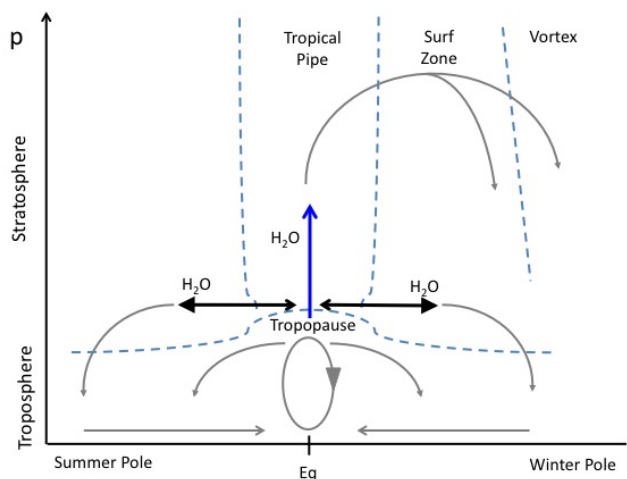
Fig. 1. Schematic of the Brewer–Dobson circulation in the stratosphere. In the lowermost stratosphere equatorial air is transported and mixed towards both poles (thick black arrows) before it re-enters the troposphere at higher latitudes and returns towards the Equator (Eq). The rising air masses in the tropics are transported towards the winter pole higher up, cross the tropical pipe and descend into the "surf zone" and the polar vortex. We focus on the three branches highlighted by the thicker blue and black arrows which distribute H_2O in the stratosphere. The ellipse and the two poleward directed arrows represent the Hadley circulation in the troposphere.

(Plumb, 2002). Stratospheric air returns to the troposphere at higher latitudes and is ultimately brought back into the tropics (equatorward arrows inside troposphere), where it joins the tropospheric Hadley-cell with upwelling in the tropics and descent in the subtropics to form the subtropical ridge.

Haynes et al. (1991) explained that the BDC is driven by breaking of high-latitude vertically propagating planetary and gravity waves which slow down the stratospheric zonal mean flow and induce a meridional residual circulation. The planetary wave breaking occurs mainly in the "surf zone" depicted in Fig. 1. However, more and more evidence from re-analysis data and model studies suggests that the upwelling in the lower tropical stratosphere is a combination of mid- to high-latitude wave breaking and the dissipation of tropical waves. Garny et al. (2011) show that slow and large scale upwelling is driven by wave forcing both in tropics and extra-tropics. Boehm and Lee (2003) state that TTL upwelling is generated as a response to poleward propagating Rossby waves that are driven by tropical convection. Randel et al. (2008) found that both equatorial planetary waves and waves originating from the extra-tropics create horizontal eddy momentum flux convergence which forces upwelling across the tropical tropopause. Using a simple model Chen and Sun (2011) showed that the planetary wave forcing in the winter tropical and subtropical stratosphere contributes most to the seasonal cycle of tropical stratospheric upwelling rather than the high-latitude wave forcing.

On the other hand Randel et al. (2002a,b), Ueyama and Wallace (2010) and Dhomse et al. (2008) showed direct evidence of the correlation of high-latitude planetary wave breaking and the strength of the BDC by using mid-latitude eddy heat flux as a proxy for wave breaking. A stronger BDC leads to lower tropical tropopause temperatures (Randel et al., 2006) and to stronger freeze drying of the stratosphere (Dhomse et al., 2008) i.e., lower H_2O concentrations. Knowledge of the BDC is, thus, crucial to determine the budget of H_2O and other atmospheric trace gases in the stratosphere since it has an important influence on the stratospheric entry, the residence time and ozone depletion. The BDC has been varying since observations started in the 1960s (Roscoe, 2006). General circulation models (GCM) predict that in a warmer climate the mass exchange between the tropics and extra-tropics will increase (Butchart et al., 2006; McLandress and Shepherd, 2009; Okamoto et al., 2011). The predicted enhancement of the BDC is due to an increase in planetary wave drag in the extra-tropical stratosphere as well as to an upward shift of the orographic gravity wave drag at low and mid-latitudes. A change in the BDC will in turn also affect stratospheric H_2O and ozone abundance.

Observational studies about the BDC variability are rare. Engel et al. (2009) showed by using balloon-borne measurements of stratospheric trace gases that the stratospheric mean age of air was slightly increasing rather than decreasing although no statistically significant trend could be extracted. This result disagrees with model predictions for a strengthening of the BDC and an associated decrease in the mean age of air. Several previous studies used the H_2O tape recorder signal to derive the ascent rate in the tropical lower stratosphere as a measure for the upwelling branch of the BDC (Mote et al., 1996; Schoeberl et al., 2008; Niwano et al., 2003; Fujiwara et al., 2010). The tropical H_2O tape recorder is displayed in Fig. 2 and shows the imprinted seasonal cycle of H_2O around the 100 hPa level which is then transported upward by the slow BDC ascent. Fujiwara et al. (2010) and Niwano et al. (2003) showed the seasonality and a clear modulation of the ascent rate by the Quasi Biennial Oscillation (QBO) using radiosonde measurements and HALOE satellite measurements, respectively. The QBO is a dynamic phenomenon in the equatorial stratosphere and manifests itself by a quasi periodic oscillation ($\cong$28–29 months) of the zonal wind between westerlies and easterlies. The alternating winds propagate downward from the stratopause (1 hPa, $\sim$55 km) at a rate of about 1 km per month towards the tropical tropopause (100 hPa, $\sim$16.6 km). The ascent rate of the tape recorder is modulated by the QBO and speeds up during the colder easterly phase and slows down during the warmer westerly phase (Niwano et al., 2003; Plumb and Bell, 1982). The ascent rate is thus anti-correlated with the temperature. As a consequence the strength of the BDC determines stratospheric H_2O entry values by modulating TTL temperatures. The QBO affects also the meridional wind. In fact, it

H$_2$O deviation from mean 8°S-8°N

%
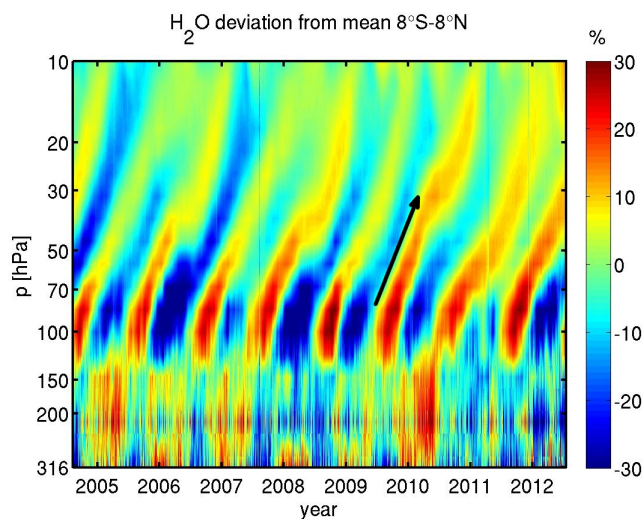
Fig. 2. The so called atmospheric tape recorder shows zonal mean H$_2$O anomalies in the tropics as a function of time and altitude. Red colours show above average volume mixing ratios, blue shows lower values mainly during NH winter near 100 hPa. The seasonal cycle with an amplitude of about 30 % is imprinted at 100 hPa and slowly transported upward by the ascending branch of the BDC as indicated by the arrow. The slope of the arrow indicates the average speed of the tropical upwelling. The variability between 316 and 150 hPa is mostly due to ENSO. In El Niño (La Niña) years more (less) H$_2$O is observed.

induces a secondary meridional circulation due to thermal wind balance, which affects the meridional branch of the BDC (Plumb and Bell, 1982; Baldwin et al., 2001; Ribera et al., 2004; Punge et al., 2009). More about the QBO can be found in Baldwin et al. (2001) and references therein.

The above mentioned work focused on seasonal and interannual variations in the tropical upwelling branch of the Brewer–Dobson circulation. By using Aura/MLS measurements we add observations of the speed of the shallow meridional branch at 100 hPa and concentrate on its link to the tropical upwelling branch of the BDC as highlighted by the thick arrows in Fig. 1. We use the rate of horizontal mixing and transport of H$_2$O to mid-latitudes as a proxy for the shallow meridional branch. For simplification we will call it the meridional speed of the BDC although it has to be pointed out that the speed derived from the meridional propagation of H$_2$O anomalies does not provide an absolute measure for the net transport of mass by the BDC. This is in contrast to the tape recorder signal which consists primarily of mass advection. The horizontally propagating anomalies we observe are due to a combination of residual mass transport and two-way mixing. Hence, the derived speed depends on the used tracer, but is a qualitative measure of the BDC. However, poleward residual mass transport is dominating. Trepte et al. (1993) used SAGE II satellite observations of stratospheric aerosols from the Mount Pinatubo (15° N, 120° E) eruption in 1991 to

characterise the stratospheric circulation. Their results show that aerosols were predominantly moved poleward and show no signs of mixing back to their tropical origin in the lower stratosphere.

Flury et al. (2012) showed that total water (ice and vapor) is roughly constant in the tropical tropopause layer (TTL) at 100 hPa on seasonal time scales. However, the temperature determines the balance between ice in cirrus clouds and water vapour. Thus, the strong seasonal cycle of temperature manifests itself also in water vapour and ice and can be found in water vapour throughout the lower stratosphere from tropics to mid-latitudes due to transport by the BDC. The slow residual transport of air out of the lower tropical stratosphere leads to a time lag in the H$_2$O time series at higher latitudes and altitudes because lower stratospheric H$_2$O concentrations are set in the tropics. This time lag enables us to retrieve the average speed of the BDC thanks to the tracer characteristics of H$_2$O. The method allows us to investigate the difference between the Northern (NH) and Southern Hemisphere (SH) by considering the different amplitude of the interannual variability of the respective meridional branch. Furthermore, we link the derived speeds to temperature and zonal wind variability. The article is organised as follows. Section 2 describes the utilised satellite and reanalysis data as well as the correlation method. Section 3 outlines the results, especially the interannual speed variations and their link to temperature and zonal wind. Section 4 discusses the QBO's effect on the tropical pipe and how we interpret the results. Finally we conclude and summarise our findings in Sect. 5.

2 Data and method

In this study, we analyse measurements from the MLS (Microwave Limb Sounder) instrument which is flown on board the Aura spacecraft and part of the NASA A-train satellite constellation. MLS measurements began in August 2004 and continue since. We use daily mean H$_2$O, ozone (O$_3$) and temperature data of version 3.3. Approximately 3500 H$_2$O profiles are retrieved on a daily basis from 316 hPa to 0.0002 hPa between 82° S and 82° N. MLS has a horizontal resolution of 200–300 km along track, 7 km across track and 3–4 km in the vertical. In this study we will focus on the lower stratospheric pressure levels of 100 hPa, 82 hPa, 68 hPa, 56 hPa, 46 hPa, 38 hPa, 32 hPa, 26 hPa, 22 hPa and 18 hPa on which MLS profiles are retrieved. The precision and accuracy of H$_2$O at 100 hPa is 10 % and 8 %, respectively (Read et al., 2007). The MLS temperature product is retrieved from 316 hPa to 0.001 hPa and interpolated on the same horizontal grid as H$_2$O for the purpose of the study. It has a vertical resolution of about 5 km at 100 hPa decreasing to 3 km in the middle stratosphere. The precision at 100 hPa is 0.8 K whilst the uncertainty is about 2 K (warm bias to other instruments such as CHAMP and AIRS/AMSU Schwartz et al., 2008). MLS O$_3$ is measured using a radiometer at 240 GHz. Profiles are

reliable between the pressure levels 215 hPa and 0.02 hPa with a vertical resolution of 2.7 to 3 km from the upper troposphere to the mid-mesosphere (Froidevaux et al., 2008). To compare our observations with the QBO we use the National Centers for Environmental Prediction/National Center for Atmospheric Research (NCEP/NCAR) reanalysis daily zonal wind data, which are retrieved on 17 pressure levels from 1000 hPa to 10 hPa. The method used to determine vertical and meridional speeds of the BDC is similar to the one introduced by Schoeberl et al. (2008) and Flury et al. (2012). We calculate the time lagged correlation in the H_2O time series between two different levels. The average speed is then determined by the ratio of the distance between the two levels and the calculated optimal time lag. In order to obtain a time series of the average speed we use a one year time window for correlation and shift one level in time with respect to the other until a maximum correlation is reached. In choosing such a 1 yr time window for correlation seasonal variations cancel out and interannual variations are emphasised. This correlation procedure is repeated every day until the end of the measurement time series. Thus, each daily value of the derived speed time series represents the average speed over the following 365 days. For the vertical upwelling speed we focus on the 68 hPa and 56 hPa levels at the Equator which are separated on the average by 1.12 km. The distance between the two pressure levels is determined with the MLS version 3.3 geopotential height data (Schwartz et al., 2008), which were averaged over the respective time period of interest. We choose this altitude to make sure to be completely above tropical convection. To evaluate the speed of the shallow meridional branch, we correlate the 100 hPa levels at the Equator and 40° latitude North and South, respectively. We use this speed as a proxy for the shallow branch knowing that the derived absolute speed is tracer dependent. We focus on the 100 hPa level because above 68 hPa H_2O loses its distinctive tracer capabilities towards the mid-latitudes due to the so called tropical pipe (Plumb, 1996) which is stronger than in the lower stratosphere and inhibits mixing more effectively. We estimate the uncertainty of the derived speeds to be 5 %. The main contributor is the uncertainty in the determination of the optimal time lag, which is about 2 days in the here shown analysis.

3   Results

3.1   Water vapour transport

Due to its long chemical lifetime of the order of tens of years in the lower stratosphere (Brasseur and Solomon, 2005) H_2O can be used as a tracer for atmospheric transport given spatial gradients of concentrations in this region. Gradients exist in our region of interest as well in the vertical at the Equator as on the horizontal between tropics and mid-latitudes in the lower stratosphere.
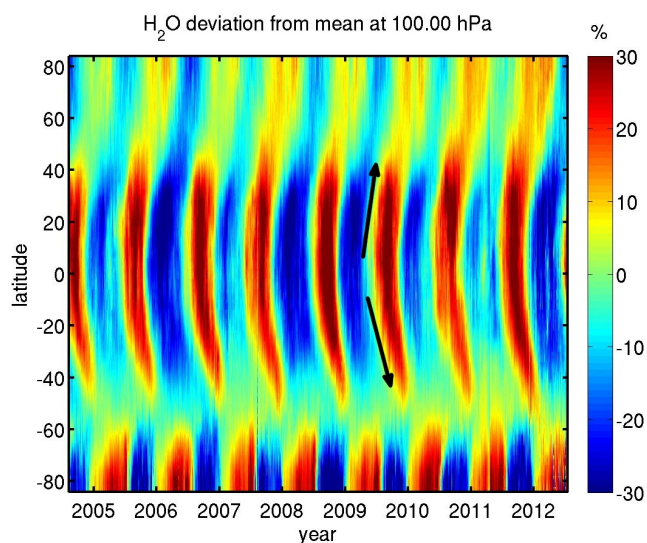
Fig. 3. Relative deviation from the average zonal mean H_2O as a function of time and latitude at 100 hPa. Red colours show above average concentrations, blue shows below average values. The visible seasonal cycle with an amplitude of about 30 % is transported from the tropics towards the poles by the meridional BDC as indicated by the arrows and can be identified along the slant lines of same colours. The slope is steeper towards the NH which is indicative for a stronger and faster BDC.

Tropical zonal mean H_2O profile time series are suitable to visualise vertical transport mechanisms. Figure 2 shows the well known atmospheric tape recorder (Mote et al., 1996) as the pressure-time series of H_2O deviations from its time mean at each pressure level. The seasonal cycle of H_2O at 100 hPa is imprinted and transported upward by the ascending branch of the BDC highlighted by the arrow. The signal is visible up to 10 hPa. Short term interannual variations in H_2O are produced by the QBO and El Niño Southern Oscillation (ENSO). Minimum values at 100 hPa occur during NH winter. The irregular interannual variability between 200 hPa and 100 hPa follows the ENSO signal. During El Niño the atmosphere is warmer and carries more H_2O (red) e.g., in 2005, 2007 and 2010. A strong La Niña occurred in 2007–2008 and 2010–2012 where H_2O is well below the average (blue). The variable speed of the ascending air masses can be estimated by computing the slope of the alternating coloured surfaces above 100 hPa highlighted by the arrow.

Figure 3 shows latitude-time series of H_2O deviations from its zonal mean at 100 hPa. The seasonal cycle is clearly visible over the whole latitude range. Red colours represent higher than average H_2O whilst blue shows lower than average values. Furthermore, we observe that the alternating bands of positive (red) and negative (blue) H_2O anomalies propagate towards the high-latitudes which is highlighted by the two arrows representing the shallow meridional branch of the BDC as previously shown in Fig. 1. The arrow is steeper

in the NH which means a faster transport, hence, a stronger BDC. The negative anomalies at high southern latitudes in the second half of each year stem from the very cold Antarctic polar vortex and the buildup of polar stratospheric clouds which dehydrate the 100 hPa level.

3.2 BDC speed variations

To compute the average speed of the vertical upwelling branch of the BDC as highlighted by the thick upward pointing arrow in Fig. 1, we correlate the time series of the 68 hPa ($\sim$18.80 km) and 56 hPa ($\sim$19.92 km) level in one year windows over the whole MLS time series. Correlation is strong with coefficients $r \sim 0.9$. Since the tape recorder signal is ascending, the H_2O at 56 hPa is lagged in time with the one at the lower level. We determine the optimal time lag in order to get maximum correlation between the two levels. Thus, the ascent rate can be computed from the ratio of the mean distance between the two levels ($\Delta z \sim 1.12$ km) and the optimal time lag. The same calculation is done for the meridional component, which constitutes the shallow branch of the BDC. We compute the time lagged correlation between the 100 hPa levels at the Equator and 40° N and 40° S ($\Delta y \sim$ 4440 km), respectively. Correlation coefficients are also generally high with $r \sim 0.9$. The uncertainty of the method is composed of the uncertainty in the distance between the levels ($\sim 2\%$) and the precision of the time lag ($\sim \pm 2$ day). The two sum up to about 5% uncertainty in the derived speed which is significantly smaller than the interannual variability of 21% found in the study. As already pointed out in the introduction, we compute the speed of the poleward propagating water vapour anomaly. Since this does not result from a pure transport process of mass, but includes two-way mixing the speed is tracer dependent. However, since poleward residual mass transport is dominant (Trepte et al., 1993) our signal is a good proxy for the speed of the BDC and for simplicity we just call it speed of the meridional branch. Figure 4 shows the results of the mean upwelling- and meridional speeds of the BDC derived from the correlation of H_2O time series. Note that the speed v in both hemispheres is taken positive towards either pole. The meridional transport in the NH (v, NH on the order of $1 \, \mathrm{m \, s^{-1}}$) is about 5000 times faster than the vertical ascent (w) which is $\sim 0.2 \, \mathrm{mm \, s^{-1}}$. The speed towards the SH (v, SH) is about half the one in the NH, which confirms the interpretation of Fig. 3 with a slower BDC in the SH. Also the austral variability of about 10% is half the variability in the NH (21%). The variability in the vertical ascent ($\sim 21\%$) is very similar to the one in the meridional to the NH. Furthermore, there is a prominent ~ 2 yr oscillation in v_NH and w which is linked to the well studied QBO. However, the observed anti-correlation of the two BDC branches in the NH was rather surprising. When the vertical upwelling branch speeds up, the meridional slows down. Both are part of the BDC, but show opposite interannual variations. Section 3.4 will discuss these particular findings in more detail.
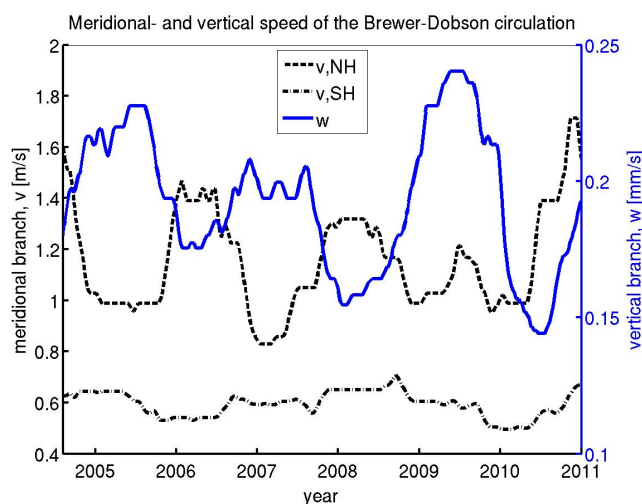
Fig. 4. Speed of the meridional branch of the BDC at 100 hPa to the NH (v, NH dashed black) and to the SH (v, SH, dashdotted black) indicated on the left axis. The equatorial vertical ascent rate (w, solid blue) at 68 hPa is shown on the right axis. Speeds show a prominent ~ 2 yr oscillation related to the QBO. Both v, NH and w show interannual variability of about 21%. The vertical speed increases in phase with a meridional speed decrease and vice versa. The speed to the SH shows less variability and is out of phase with the NH for the most part, except for the first 3 yr where they are correlated.
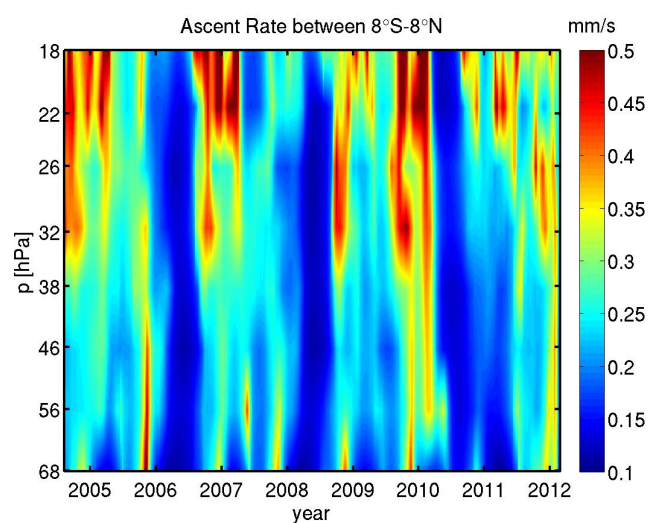
Since we use one year increments of H_2O data for correlation we do not retrieve the typical seasonal variation of the Brewer–Dobson circulation which is picking up in the months September to March every year due to enhanced high-latitude stratospheric wave breaking. Niwano et al. (2003) showed time series of vertical ascent rate profiles using HALOE H_2O and CH_4 data where the seasonal cycle is visible with maxima occurring during NH winter. To verify the Niwano et al. (2003) results, we determine the time it takes for an air parcel to ascend by one pressure level using MLS daily zonal mean H_2O data averaged between 8° S–8° N. We are specifically investigating the time it takes to shift a lower stratospheric segment of a profile up by one MLS pressure level as can be identified in Fig. 5. Thereby, we determine the number of days j it takes to obtain the best correlation of the 100 hPa to 56 hPa profile at time t_i (left blue) with a profile taken one MLS pressure level higher up i.e., from 82 hPa to 46 hPa at a time t_{i+j} (right blue). This calculation is repeated for every day and subsequent pressure levels up to 10 hPa in order to get a time series of the average vertical ascent rate profile at a higher temporal resolution. We use MLS geopotential height data to compute the average height difference between the considered levels. The increasing spacing with altitude between the levels shown in Fig. 6 (from $\Delta z = 1.11$ km to $\Delta z = 1.31$ km) is taken into account. The ascent rate is, thus, derived by the covered distance divided by the computed time lag. The speed is attributed to
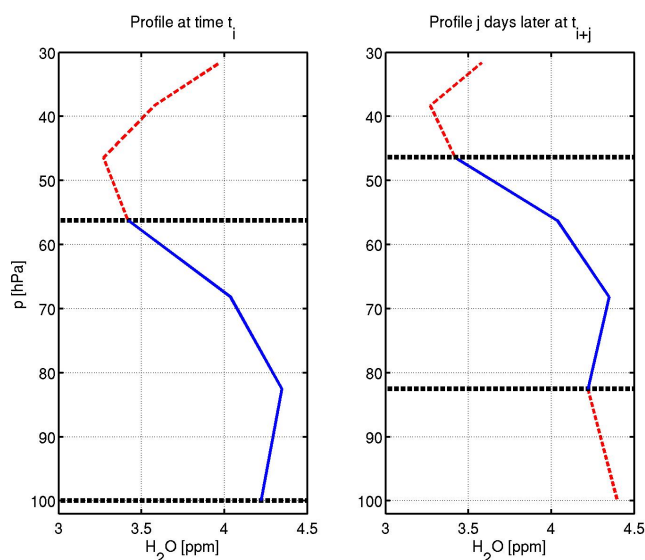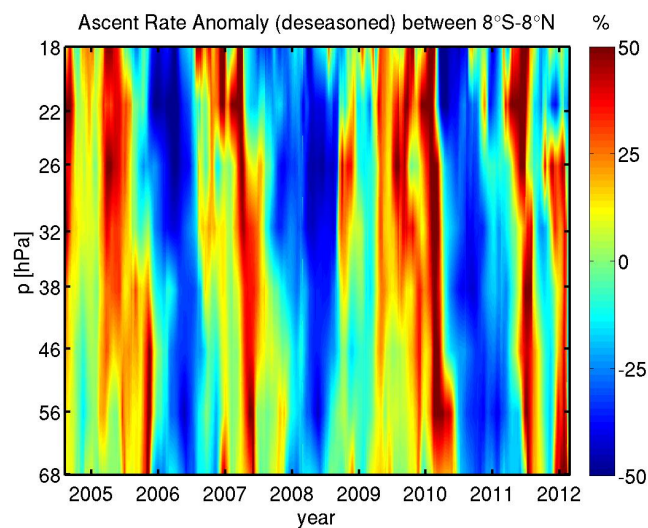
Fig. 5. Schematics on how the vertical ascent rate is computed using the Niwano et al. (2003) method. A portion of a H_2O profile is taken at a time t_i between 100 hPa and 56 hPa (left, blue). Due to BDC ascent the profile will be shifted upward some time later. At a specific time t_{i+j}, j days later, the structure can be found one pressure level higher up (right, blue). In order to compute this time, we correlate the blue H_2O segment on the left with the segment one level higher up (right, blue) on subsequent days until maximum correlation is reached after j days. The ratio of the ascended distance and the time lag j yields the average ascent rate.

Fig. 6. Average vertical speed in the lower stratosphere between 68 hPa ($\sim$ 18.8 km) and 18 hPa ($\sim$ 27.2 km) as a function of time calculated according to Niwano et al. (2003). A seasonal cycle is apparent with higher speeds (red) increasing with altitude and towards the end of each calendar year during NH winter, which is consistent with the characteristics of the BDC which is strongest from September to March. During NH summer the vertical speed decreases (blue) due to the reduced planetary wave breaking, which is the main driver of the BDC.

the centre pressure level of the considered altitude layer. Figure 6 shows the time series of ascent rate profiles in the lower stratosphere between 68 hPa ($\sim$ 18.8 km) and 18 hPa ($\sim$ 27.2 km). The speed varies between about 0.1 mm s^{-1} and 0.5 mm s^{-1} with maximum values occurring usually during the NH autumn and winter months when the BDC is stronger. The values are greater than those obtained with the previous method because of the better time resolution which allows us to identify the seasonal cycle of the BDC. The average speed in the considered altitude range is about 0.24 mm s^{-1} which again compares well to Fig. 4 taking into account the small increase of speed with altitude. However, to better compare the data with the vertical speed shown in Fig. 4, we compute the anomalies by removing the seasonal cycle which is shown in Fig. 7. Again, we observe a strong QBO signal which slowly descends with a speed of about 1– 1.5 km month^{-1} from the upper boundary of the plot. Lower ascent rates are observed in 2006, 2008 and 2010–2011. The variability of about 50 % is bigger than observed in Fig. 4 and is due to the different method used to compute the speed.

Table 1 shows an overview of our ascent rates in the lower stratosphere at six different pressure levels together with data published by Niwano et al. (2003), Mote et al. (1996) and Schoeberl et al. (2008). The values are extracted from the figures in the corresponding publications. Our values represent
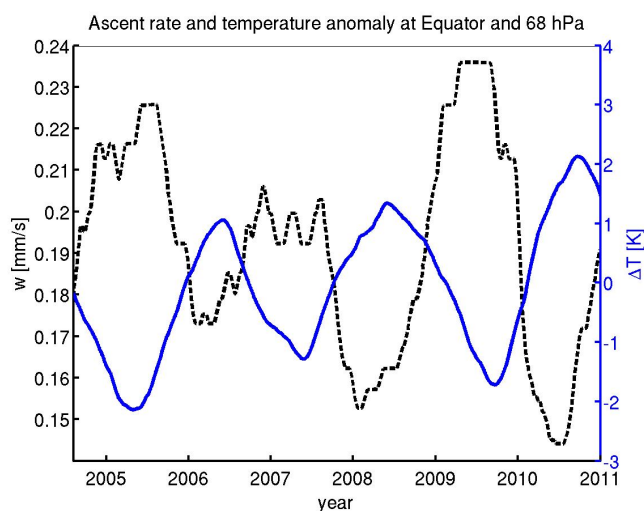

Fig. 7. Anomalies of the ascent rates shown in Fig. 6 with the seasonal cycle removed. A distinct $\sim$2 yr cycle is visible which is descending slowly at a rate of about 1.5 km month^{-1}. The variability is about 50 % with lower ascent rates (blue) observed in 2006, 2008 and 2010–2011. The negative anomalies occur during the QBO westerly phase as will be shown in Fig. 10. Periods of faster upwelling are indicated in red.

Table 1. Comparison of tropical ascent rates w [mm s^{-1}] in the lower stratosphere from different studies. Niwano et al. (2003) and Mote et al. (1996) used HALOE satellite observations and averaged between $\pm 12.5°$, Schoeberl et al. (2008) used a combination of 15 yr of HALOE and Aura/MLS H$_2$O observations to compute w at the Equator. They also displayed results of the GEOS-4 general circulation model. Ascent rates are increasing with altitude and very similar to each other. However, the GEOS-4 model underestimates the observations. The slow tropical ascent is in contrast to the faster meridional speed (~ 1 m s^{-1}).

p [hPa]	$\sim z$ [km]	This Study w [mm s^{-1}]	Niwano 03 w [mm s^{-1}]	Mote 96 w [mm s^{-1}]	Schoeberl 08 w [mm s^{-1}]	GEOS-4 GCM w [mm s^{-1}]
70	18.7	0.20			0.30	0.12
60	19.6	0.22	0.22	0.20	0.30	0.12
50	20.7	0.22	0.24	0.22	0.30	0.15
40	22.0	0.23	0.25	0.25	0.32	0.19
30	23.8	0.27	0.28	0.30	0.35	0.25
20	26.4	0.31	0.33	0.40	0.50	0.36

Fig. 8. The vertical ascent rate at the Equator between 68 hPa and 56 hPa (dashed black, left y-axis) is compared to the MLS temperature anomaly (solid blue, right y-axis) at the same latitude and pressure. The temperature time series has been smoothed by a one year forward moving average to match the method which is used to determine the ascent rate. Each value represents the average over the next year. Temperature is anti-correlated with the vertical ascent as expected.

the average of the data shown in Fig. 6 at corresponding pressure levels. All studies agree on the increase with altitude and the values agree well among each other. Taking into account the respective uncertainties (~ 5–25 %) given in the publications the range of values overlap. Furthermore, Schoeberl et al. (2008) who obtained the highest values using a combination of HALOE and Aura/MLS H$_2$O show also the highest standard deviation. In their work they compared the ascent rates with the GEOS-4 general circulation model which shows overall the lowest values. The slow ascent rate is in contrast with the much faster meridional speed of ~ 1 m s^{-1}.

3.3 Link of temperature and vertical ascent

The speed of the BDC circulation plays a key role in steering the tropical tropopause temperature as well as the temperature in the lower stratosphere. An increase in speed of the BDC leads to a cooling of the tropical tropopause and the stratosphere as was already shown by Niwano et al. (2003); Randel et al. (2006); Yulaeva et al. (1994). Triggered by enhanced upwelling, the reaction of the temperature is a combination of adiabatic cooling and ozone decrease due to advection of lower ozone concentrations from below (Yulaeva et al., 1994; Randel et al., 2006). Less ozone results in less radiative heating. In order to compare our time series of the ascent rate (see Fig. 4) with the temperature anomalies at the same latitude and pressure we need to compute a moving average over a one year period since the calculated speeds represent the average over the following year. Figure 8 shows the time series of the MLS temperature anomaly at the Equator and 68 hPa smoothed by a one year forward moving average in blue and the ascent rate in dashed black. Each point in the time series represents the average over the next year. As expected, an increase of the vertical velocity is accompanied by a decrease in temperature. Clearly visible again is the QBO modulation producing the ~ 2 yr cycle. The expected anti-correlation between the temperature and the vertical ascent can be seen as a validation of our method to compute the speed of the BDC.
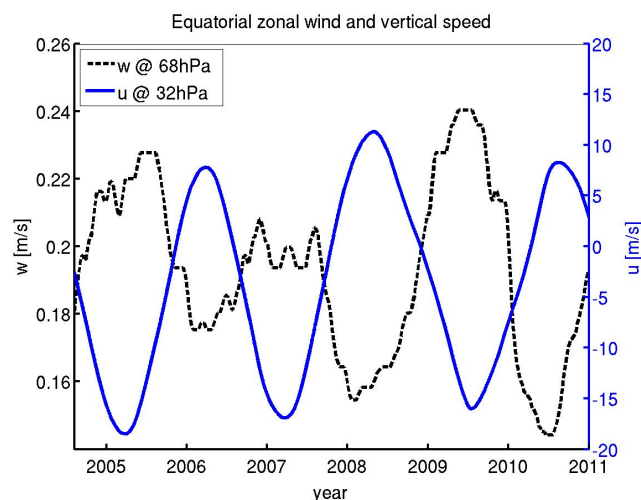
3.4 QBO influence on BDC

The QBO is associated with a secondary meridional circulation anomaly that does not only affect the residual transport to mid-latitudes, but also the vertical ascent in the tropical stratosphere (Reed, 1964; Plumb and Bell, 1982; Choi et al., 2002; Punge et al., 2009; Ribera et al., 2004). Figure 9 shows schematically the QBO associated circulation anomaly as a latitude-height section on the left and the vertical profile of the equatorial zonal wind u on the right. Below the maximum easterlies (E) there is enhanced vertical ascent
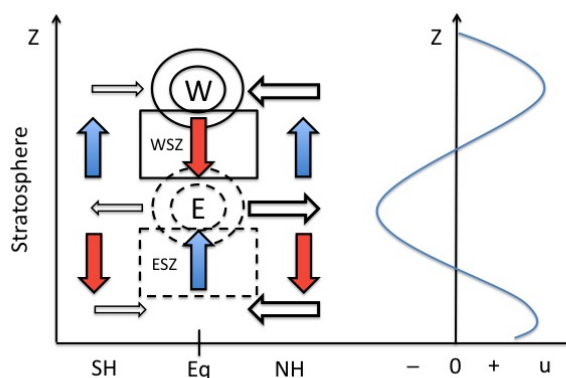
Fig. 9. Sketch of the QBO secondary meridional circulation on the left and the zonal wind profile at the Equator on the right. Arrows indicate vertical and meridional motion with colours meaning warming (red) and cooling (blue). Below the altitude of maximum easterlies (E) air is rising faster in the easterly shear zone (ESZ). At the altitude of maximum easterlies air is diverging towards the poles and increases the speed of the BDC, the opposite is found at the altitude of maximum westerlies (W) where air converges at the Equator (Eq) and leads to downdrafts below that level which decrease the speed of the ascent and warm the atmosphere inside the westerly shear zone (WSZ). From our results of the hemispheric asymmetry in the meridional BDC-branch we conclude that the secondary meridional circulation is less strong in the SH by a factor of 2 and reduced the arrows accordingly in size. Figure adapted from Choi et al. (2002); Plumb and Bell (1982); Punge et al. (2009).


Fig. 10. Ascent rate w at the Equator between the 68 and 56 hPa level (dashed black, left y-axis) together with the average equatorial zonal wind u (solid blue, right y-axis) higher up at 32 hPa. In order to compare to the ascent rate the zonal wind is smoothed with a one year forward moving average. The data confirm the sketch in Fig. 9 and show maximum ascent rates during the easterly phase ($u < 0$) and minimum during the westerly phase ($u > 0$).

inside the easterly shear zone (EZS), which is associated with lower temperatures. At the altitude of maximum easterlies (E) we find meridional divergence towards the poles. Inside the westerly shear zone (WSZ) just below the maximum westerlies (W) we find a descent anomaly, which is associated with higher temperatures and reduces the speed of the prevailing BDC ascent. At the height of maximum westerlies we find a meridional convergence zone at the Equator. We adapted the sketch from Choi et al. (2002) and Punge et al. (2009) who drew two symmetrical cells separated by the Equator. However, Peña-Ortiz et al. (2008) report on an asymmetry in autumn and spring when there is only one cell which is shifted completely into the winter hemisphere. Our results also suggest an asymmetry in the meridional components since the interannual variability of the meridional branch towards the NH is twice as strong as to the SH (see Fig. 4). For this reason we adapted the size of the meridional arrows to highlight the asymmetry. To sum up, easterly winds are associated with cold anomalies and higher vertical ascent rates below the level of maximum easterlies whilst westerly winds are associated with warm anomalies and lower vertical ascent rates below the level of maximum westerlies.

To compare the theory of Fig. 9 with MLS measurements we compare the ascent rate with the zonal wind of a level higher up. In our case we choose the ascent rate calculated between the levels 68 hPa and 56 hPa and the average zonal

wind at the 32 hPa level, both time series are taken at the Equator. The results are displayed in Fig. 10. The ascent rate is plotted in black (dashed) and varies between 0.14 mm s^{-1} and 0.24 mm s^{-1}. The NCEP average zonal wind (solid blue) is anti-correlated ($r = -0.84$) with the ascent rate and confirms the schematics of Fig. 9. The ascent rate starts increasing right after maximum westerlies- and decreases after the maximum easterlies are reached. The upward motion is slowest during the westerly wind regime. Note that even during the westerlies the ascent rate is positive, the red downward arrow in Fig. 9 only indicates the QBO induced anomaly which slows down the prevailing upward motion but does not reverse it.

Figure 11 shows the same zonal wind time series as the previous figure, but together with the average meridional speed between the Equator and 40° N at 100 hPa. The zonal wind speed correlates with the meridional speed, the correlation coefficient here is $r = 0.73$. This behaviour can also be explained with the sketch in Fig. 9. The considered 100 hPa level for meridional transport is well below the 32 hPa of the zonal wind and, for example, in the case of maximal eastward wind (E in Fig. 9) the converging arrows in the lowest part of the figure apply which slow down the transport towards the poles. During the westerly phase, the meridional transport gets faster below, which also applies to our case here.
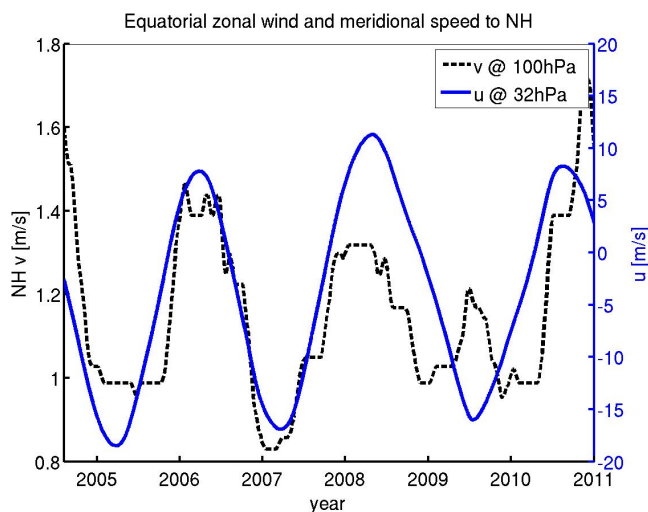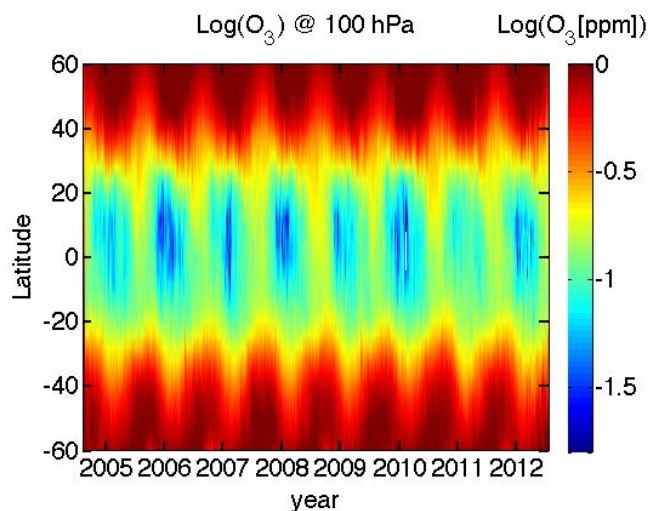
Fig. 11. Speed of the meridional branch (dashed black, left y-axis) of the BDC to the NH at 100 hPa and the average equatorial zonal wind at 32 hPa (solid blue, right y-axis). The meridional speed is in phase with the wind and increases (decreases) as suggested by Fig. 9 during the westerly/positive (easterly/negative) phase of the zonal wind u.

Fig. 12. Logarithm of zonal mean MLS O_3 volume mixing ratios (ppm) at 100 hPa. O_3 rich air from mid-latitudes (red-orange) is mixed into the tropics especially in NH summer and autumn. During winter and spring the low O_3 concentrations (blue) in the tropics are more isolated because mixing equatorwards is strongly reduced.

4 Discussion

With our time lagged correlation method using water vapour time series we derived the speed of the vertical upwelling branch of the BDC at the Equator as well as a proxy for the speed of the shallow meridional branch. For reasons of simplicity, we use the term meridional speed for the derived signal although it is tied to the used tracer H_2O. Whilst the tape recorder signal (tropical upwelling) represents a slow diabatic ascent and is due to vertical mass advection the meridional transport in the shallow branch is a combination of residual (poleward) mass transport and two-way mixing. The correlation of H_2O at 100 hPa between 40° S/N and the Equator is, thus, more regarded as a proxy for the speed of the shallow meridional component rather than an absolute measure of the speed. The reason for this is two-way mixing and the considered tracer gradient field, which determines diffusion. However, since the considered propagation of the H_2O anomaly between the Equator and 40° is predominantly due to poleward residual mass transport (Trepte et al., 1993), we consider it as a good proxy for the shallow branch of the BDC. Two-way mixing, which is faster in NH summer and autumn (Bönisch et al., 2009; Birner and Bönisch, 2011; Hegglin and Shepherd, 2007), can be observed in an O_3 time-latitude plot at 100 hPa shown in Fig. 12 where mid-latitude air with higher O_3 concentrations enters the tropics. Nevertheless, during winter and spring the tropical lower stratosphere is much more isolated from the extra-tropics and there is no visible mixing into the tropics. However, at the same time we clearly observe H_2O transport towards the poles (Fig. 3). The mixing barrier can be identified at approx. ±20°

latitude and is referred to as the tropical pipe (Plumb, 1996). The pipe separates tropical- from mid-latitude air which can be seen in steep gradients of various trace gas distributions such as e.g., N_2O, O_3 and H_2O. The tropical pipe is stronger above 70 hPa than below where it is leaky especially during summer.

In order to monitor transport processes using H_2O as a tracer, we need an observable gradient, which exists on the 100 hPa level between the tropics and mid-latitudes. Mid-latitude H_2O at 100 hPa originates in the tropics and is mostly transported through the shallow branch of the BDC. In late winter and spring measurements show an increase in the age of lower stratospheric air which is indicative for downwelling from the deep branch of the BDC (Bönisch et al., 2009). However, this only happens over relatively short time periods. The same authors used a concept of mass balance to compute the contribution of the deep and shallow branch to extratropical lower stratospheric air and demonstrated that downwelling plays a role only during spring whereas direct horizontal transport from the tropical tropopause layer contributes during the whole year. Since we use one year time segments of H_2O to derive the meridional speed, the deep branch of the BDC does not influence our results significantly. Moreover, the meridional gradient between tropics and mid-latitudes is stronger than the vertical gradient around the 100 hPa level (100–82 hPa) so that the influence of mid-latitude vertical transport on our derived meridional speed is small.

Our results show that the QBO has a significant influence on the vertical and meridional speed of the BDC. Below the zone of maximum easterlies (QBO east) the vertical speed

increases and the meridional speed decreases. The opposite happens below the zone of maximum westerlies (QBO west) as suggested by Fig. 9. Thus, the QBO has an influence on how the upwelling air masses are distributed into the tropical stratosphere. We suggest an influence on the tropical pipe (Plumb, 1996) to explain the variability of the speed towards mid-latitudes. Figure 13 sketches the tropical pipe and Brewer–Dobson transport for the QBO easterly phase on the left and the QBO westerly phase on the right. We assume a constant vertical supply of tropospheric air that crosses the tropical tropopause during both QBO phases. The enhancement of the respective branches is highlighted by the increased and gray shaded arrows. During the easterly phase the meridional speed towards the NH is about 40 % smaller than during west. We suggest that during this time the tropical pipe is stronger and mixing with the mid-latitudes takes more time. On the other hand for continuity reasons the vertical ascent rate is increased by about 40 % (see Fig. 4) compared to the westerly phase. However, during the QBO westerly phase we observe the opposite, meridional transport is faster and vertical speed decreases. We, thus, assume that the tropical pipe is more leaky and allows for faster transport towards the mid-latitudes which in turn reduces the vertical speed because the increased meridional flux leaves less mass to be moved upward. The reason could be that the lower altitude limit of the tropical pipe varies as a function of the QBO. We assume that during QBO-west the tropical pipe starts higher up than during QBO-east which would explain the difference in the speed of mixing and transporting H_2O towards mid-latitudes.

The observed asymmetry between the meridional speed in the SH and NH is consistent with the theory of the QBO. Its influence is more visible in the NH because planetary wave activity at NH mid-latitudes, the primary driver of the BDC, depends strongly on the QBO because planetary wave propagation is a function of the variable zonal mean flow. Since planetary wave activity is lower in the SH the QBO influence on the meridional branch is small. However, as mentioned in the introduction, wave activity inside the tropical pipe (Randel et al., 2008; Kerr-Munslow and Norton, 2006; Norton, 2006; Garny et al., 2011; Engida and Folkins, 2012) has also an influence on tropical upwelling and the relative importance of both mechanisms is still a matter of debate. We suggest that modelling groups try to reproduce our observations (w and v) with the goal to quantify the relative contribution of tropical and high-latitude wave activity on the BDC by either switching on or off the different wave forcings.

Our results show that the QBO is the main driver of interannual variability in upwelling and meridional transport whilst the BDC controls the seasonal variability. On the other hand, the influence of the troposphere on the stratosphere is dominated by ENSO, which modulates the temperature and water vapour content of the troposphere particularly the tropical tropopause temperature. Nevertheless, we do not discuss ENSO in more detail since its influence on interannual
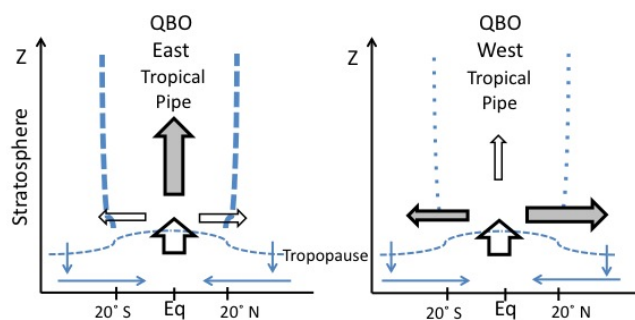
Fig. 13. Interpretation of the QBO influence on the BDC variability. During the QBO easterly phase (left) the tropical pipe is stronger and it takes more time for air masses to cross the barrier towards mid-latitudes. Thus, the meridional speed is slower. For continuity, the vertical branch has to speed up which is shown by the big shaded vertical arrow. On the other hand, during the QBO westerly phase the tropical pipe is shifted up, more leaky and transport towards the mid-latitudes faster (right). Again, for continuity reasons, the vertical transport has to slow down which agrees well with our results.

variability of the BDC is weaker than the QBO's. However, we note that ENSO and QBO get out of phase in 2009/2010 (Liang et al., 2011) which corresponds also to the time when the vertical (w) and meridional (vNH) velocity lose their anticorrelation. Whenever ENSO and QBO occur in phase the signatures on TTL- and lower stratospheric water vapour are the most prominent. Yet, a detailed analysis would require to understand the effects of the interaction of QBO and ENSO which is beyond the scope of this study.

5   Conclusions

We used the water vapour tape recorder signal to derive the speed of the tropical upwelling branch of the BDC from 7 yr of Aura/MLS measurements. In a similar way, we computed a proxy for the speed of the shallow meridional branch of the BDC in the lowermost stratosphere of both hemispheres. We found that the interannual variability of the BDC speed depends on the phase of the QBO. The tropical upwelling branch as well as the meridional branch towards the NH show interannual amplitudes of about 21 % whereas the SH meridional branch is less variable. The average speed to the NH is $1.15\,\mathrm{m\,s^{-1}}$ with an amplitude of $0.24\,\mathrm{m\,s^{-1}}$ whilst it is only $0.58\,\mathrm{m\,s^{-1}}$ with an amplitude of $0.06\,\mathrm{m\,s^{-1}}$ to the SH. The tape recorder signal ascends with an average speed of $0.20\,\mathrm{mm\,s^{-1}}$ with an amplitude of $0.04\,\mathrm{mm\,s^{-1}}$ in the lower stratosphere at the Equator. When using the method to retrieve short term variability of the vertical ascent we found maximum values of $0.5\,\mathrm{mm\,s^{-1}}$ during NH winter higher up at 20 hPa. Moreover, we found that the variability in the meridional (NH) and vertical branch are anti-correlated. This anti-correlation is regulated by the so called QBO secondary

meridional circulation which is sketched in Fig. 9. We suggest that during the QBO easterly phase the tropical pipe is stronger and it takes more time for tropical air masses to mix into mid-latitude air. However, during the QBO westerly phase the tropical pipe appears more leaky and meridional transport is faster. We suggest that the lower altitude limit of the tropical pipe is higher up during QBO-west. Our method was able to show the asymmetry of NH and SH and the different influence of the QBO on the BDC. If used by modellers our results may help to quantify the relative importance of tropical wave dissipation and high-latitude wave breaking on the BDC.

MLS temperature measurements confirm the anti-correlation between temperatures and vertical speed and show cooling (warming) during the easterly (westerly) shear phase while vertical speed is higher (lower) and meridional speed is lower (higher) (Fig. 8). NCEP/NCAR zonal wind reanalysis data also show the influence of the QBO on the tropical upwelling and meridional branch of the BDC. Strong easterlies lead to faster vertical ascent whilst westerlies reduce the ascent rate (Fig. 10). On the other hand, westerlies higher up increase the meridional speed at the 100 hPa level, whereas it is lower during the easterly phase (Fig. 11). However, since the QBO secondary meridional circulation is a function of altitude and time the conclusions derived here are based largely on MLS observations at 100 hPa and 68 hPa. We suggest that further studies concentrate on the meridional branch of the BDC higher up in the stratosphere using H_2O and methane (CH_4) data. H_2O alone is less suitable as a tracer for horizontal transport above 68 hPa due to the oxidation of CH_4 which is a significant source of H_2O in the stratosphere. General circulation models can be tested for the correct representation of the atmospheric tape recorder. The underlying H_2O distribution in the upper troposphere and the seasonal cycle is crucial for a correct representation, a task where most models still perform poorly as noted by Jiang et al. (2012). It is also difficult to find the QBO signal in the modelled tape recorder (J. Jiang, personal communication, 2012). MLS has been a very stable instrument for monitoring middle atmospheric dynamics though its primary strength is on atmospheric composition and chemistry. It is, thus, highly recommended to be used intensively for validation and improvements of global chemistry climate models since important atmospheric oscillations such as ENSO and QBO are well recorded by MLS measurements.

Edited by: W. Lahoz

References

Baldwin, M. P., Gray, L. J., Dunkerton, T. J., Hamilton, K., Haynes, P. H., Randel, W. J., Holton, J. R., Alexander, M. J., Hirota, I., Horinouchi, T., Jones, D. B. A., Kinnersley, J. S., Marquardt, C., Sato, K., and Takahashi, M.: The quasi-biennial oscillation, Rev. Geophys., 39, 179–230, doi:10.1029/1999RG000073, 2001.

Birner, T. and Bönisch, H.: Residual circulation trajectories and transit times into the extratropical lowermost stratosphere, Atmos. Chem. Phys., 11, 817–827, doi:10.5194/acp-11-817-2011, 2011.

Boehm, M. T. and Lee, S.: The Implications of Tropical Rossby Waves for Tropical Tropopause Cirrus Formation and for the Equatorial Upwelling of the Brewer–Dobson Circulation., J. Atmos. Sci., 60, 247–261, doi:10.1175/1520-0469(2003)060<0247:TIOTRW>2.0.CO;2, 2003.

Bönisch, H., Engel, A., Curtius, J., Birner, Th., and Hoor, P.: Quantifying transport into the lowermost stratosphere using simultaneous in-situ measurements of SF6 and CO_2, Atmos. Chem. Phys., 9, 5905–5919, doi:10.5194/acp-9-5905-2009, 2009.

Brasseur, G. P. and Solomon, S.: Aeronomy of the Middle Atmosphere: Chemistry and Physics of the Stratosphere and Mesosphere, Aeronomy of the Middle Atmosphere: Chemistry and Physics of the Stratosphere and Mesosphere, edited by: Brasseur, G. P. and Solomon, S., 2005, XII, 644 pp., 3rd rev. and enlarged Edn. 1-4020-3284-6, Berlin, Springer, 2005.

Brewer, A. W.: Evidence for a world circulation provided by measurements of helium and water vapour distribution in the stratosphere, Q. J. R. Meteorol. Soc., 75, 351, doi:10.1002/qj.49707532603, 1949.

Butchart, N. and Scaife, A. A. and Bourqui, M. and de Grandpré, J. and Hare, S. H. E. and Kettleborough, J. and Langematz, U. and Manzini, E. and Sassi, F. and Shibata, K. and Shindell, D. and Sigmond, M. : Simulations of anthropogenic change in the strength of the Brewer Dobson circulation, Clim. Dynam., 27, 727–741, doi:10.1007/s00382-006-0162-4, 2006.

Chen, G. and Sun, L.: Mechanisms of the Tropical Upwelling Branch of the Brewer–Dobson Circulation: The Role of Extratropical Waves, J. Atmos. Sci., 68, 2878–2892, doi:10.1175/JAS-D-11-044.1, 2011.

Choi, W., Lee, H., Grant, W. B., Park, J. H., Holton, J. R., Lee, K.-M., and Naujokat, B.: On the secondary meridional circulation associated with the quasi-biennial oscillation, Tellus Ser. B, Chem. Phys. Meteorol., 54, 395–406, doi:10.1034/j.1600-0889.2002.201286.x, 2002.

Dhomse, S., Weber, M., and Burrows, J.: The relationship between tropospheric wave forcing and tropical lower stratospheric water vapour, Atmos. Chem. Phys., 8, 471–480, doi:10.5194/acp-8-471-2008, 2008.

Dobson, G. M. G.: Origin and distribution of polyatomic molecules in the atmosphere, Proc. R. Soc. Lond. A., 236, 187–193, 1956.

Engel, A., Möbius, T., Bönisch, H., Schmidt, U., Heinz, R., Levin, I., Atlas, E., Aoki, S., Nakazawa, T., Sugawara, S., Moore, F., Hurst, D., Elkins, J., Schauffler, S., Andrews, A., and Boering, K.: Age of stratospheric air unchanged within uncertainties over the past 30 years, Nat. Geosci., 2, 28–31, doi:10.1038/ngeo388, 2009.

Engida, Z. and Folkins, I.: Upwelling into the lower stratosphere forced by breaking tropical waves: evidence from chemical tracers, Atmos. Chem. Phys. Discuss., 12, 19571–19615, doi:10.5194/acpd-12-19571-2012, 2012.

Flury, T., Wu, D. L., and Read, W. G.: Correlation among cirrus ice content, water vapour and temperature in the TTL as observed by CALIPSO and Aura/MLS, Atmos. Chem. Phys., 12, 683–691, doi:10.5194/acp-12-683-2012, 2012.

Froidevaux, L., Jiang, Y. B., Lambert, A., Livesey, N. J., Read, W. G., Waters, J. W., Browell, E. V., Hair, J. W., Avery, M. A., McGee, T. J., Twigg, L. W., Sumnicht, G. K., Jucks, K. W., Margitan, J. J., Sen, B., Stachnik, R. A., Toon, G. C., Bernath, P. F., Boone, C. D., Walker, K. A., Filipiak, M. J., Harwood, R. S., Fuller, R. A., Manney, G. L., Schwartz, M. J., Daffer, W. H., Drouin, B. J., Cofield, R. E., Cuddy, D. T., Jarnot, R. F., Knosp, B. W., Perun, V. S., Snyder, W. V., Stek, P. C., Thurstans, R. P., and Wagner, P. A.: Validation of Aura Microwave Limb Sounder stratospheric ozone measurements, J. Geophys. Res. Atmos., 113, D15S20, doi:10.1029/2007JD008771, 2008.

Fujiwara, M., Vömel, H., Hasebe, F., Shiotani, M., Ogino, S.-Y., Iwasaki, S., Nishi, N., Shibata, T., Shimizu, K., Nishimoto, E., Valverde Canossa, J. M., Selkirk, H. B., and Oltmans, S. J.: Seasonal to decadal variations of water vapour in the tropical lower stratosphere observed with balloon-borne cryogenic frost point hygrometers, J. Geophys. Res., 115, D18304, doi:10.1029/2010JD014179, 2010.

Garny, H., Dameris, M., Randel, W., Bodeker, G. E., and Deckert, R.: Dynamically Forced Increase of Tropical Upwelling in the Lower Stratosphere, J. Atmos. Sci., 68, 1214–1233, doi:10.1175/2011JAS3701.1, 2011.

Haynes, P. H., McIntyre, M. E., Shepherd, T. G., Marks, C. J., and Shine, K. P.: On the "Downward Control" of Extratropical Diabatic Circulations by Eddy-Induced Mean Zonal Forces, J. Atmos. Sci., 48, 651–680, doi:10.1175/1520-0469(1991)048<0651:OTCOED>2.0.CO;2, 1991.

Hegglin, M. I. and Shepherd, T. G.: O_3-N_2O correlations from the Atmospheric Chemistry Experiment: Revisiting a diagnostic of transport and chemistry in the stratosphere, J. Geophys. Res., 112, D19301, doi:10.1029/2006JD008281, 2007

Jiang, J. H., Su, H., Zhai, C., Perun, V. S., Del Genio, A., Nazarenko, L. S., Donner, L. J., Horowitz, L., Seman, C., Cole, J., Gettelman, A., Ringer, M. A., Rotstayn, L., Jeffrey, S., Wu, T., Brient, F., Dufresne, J.-L., Kawai, H., Koshiro, T., Watanabe, M., LEcuyer, T. S., Volodin, E. M., Iversen, T., H., D., Mesquita, M. D. S., Read, W. G., Waters, J. W., Tian, B., Teixeira, J., and Stephens, G. L.: Evaluation of Cloud and Water Vapor Simulations in CMIP5 Climate Models Using NASA A-Train Satellite Observations, J. Geophys. Res., 117, D16, doi:10.1029/2011JD017237, 2012

Kerr-Munslow, A. M. and Norton, W. A.: Tropical Wave Driving of the Annual Cycle in Tropical Tropopause Temperatures. Part I: ECMWF Analyses, J. Atmos. Sci., 63, 1410–1419, doi:10.1175/JAS3697.1, 2006.

Liang, C. K., Eldering, A., Gettelman, A., Tian, B., Wong, S., Fetzer, E. J., and Liou, K. N.: Record of tropical interannual variability of temperature and water vapour from a combined AIRS-MLS data sets, J. Geophys. Res., 116, D06103, doi:10.1029/2010JD014841, 2011.

McLandress, C. and Shepherd, T. G.: Simulated Anthropogenic Changes in the Brewer-Dobson Circulation, Including Its Extension to High Latitudes, J. Climate, 22, 1516, doi:10.1175/2008JCLI2679.1, 2009.

Mote, P. W., Rosenlof, K. H., McIntyre, M. E., Carr, E. S., Gille, J. C., Holton, J. R., Kinnersley, J. S., Pumphrey, H. C., Russell, III, J. M., and Waters, J. W.: An atmospheric tape recorder: The imprint of tropical tropopause temperatures on stratospheric water vapour, J. Geophys. Res., 101, 3989–4006, doi:10.1029/95JD03422, 1996.

Niwano, M., Yamazaki, K., and Shiotani, M.: Seasonal and QBO variations of ascent rate in the tropical lower stratosphere as inferred from UARS HALOE trace gas data, J. Geophys. Res., 108, 4794, doi:10.1029/2003JD003871, 2003.

Norton, W. A.: Tropical Wave Driving of the Annual Cycle in Tropical Tropopause Temperatures. Part II: Model Results., J. Atmos. Sci., 63, 1420–1431, doi:10.1175/JAS3698.1, 2006.

Okamoto, K., Sato, K., and Akiyoshi, H.: A study on the formation and trend of the Brewer–Dobson circulation, J. Geophys. Res., 116, D10117, doi:10.1029/2010JD014953, 2011.

Peña-Ortiz, C., Ribera, P., García-Herrera, R., Giorgetta, M. A., and García, R. R.: Forcing mechanism of the seasonally asymmetric quasi-biennial oscillation secondary circulation in ERA-40 and MAECHAM5, J. Geophys. Res., 113, D16103, doi:10.1029/2007JD009288, 2008.

Plumb, A. R. and Bell, R. C.: A model of the quasi-biennial oscillation on an equatorial beta-plane, Q. J. R. Meteorol. Soc., 108, 335–352, doi:10.1002/qj.49710845604, 1982.

Plumb, R. A.: A "tropical pipe" model of stratospheric transport, J. Geophys. Res., 101, 3957–3972, doi:10.1029/95JD03002, 1996.

Plumb, R. A.: Stratospheric transport, J. Meteorol. Soc. Japan, 80, 793–809, 2002.

Punge, H. J., Konopka, P., Giorgetta, M. A., and Müller, R.: Effects of the quasi-biennial oscillation on low-latitude transport in the stratosphere derived from trajectory calculations, J. Geophys. Res., 114, D03102, doi:10.1029/2008JD010518, 2009.

Randel, W. J., Garcia, R. R., and Wu, F.: Time-Dependent Upwelling in the Tropical Lower Stratosphere Estimated from the Zonal-Mean Momentum Budget., J. Atmos. Sci., 59, 2141–2152, doi:10.1175/1520-0469(2002)059<2141:TDUITT>2.0.CO;2, 2002a.

Randel, W. J., Wu, F., and Stolarski, R.: Changes in Column Ozone Correlated with the Stratospheric EP Flux, J. Meteorol. Soc. Japan, 80, 849–862, doi:10.2151/jmsj.80.849, 2002b.

Randel, W. J., Wu, F., Vömel, H., Nedoluha, G. E., and Forster, P.: Decreases in stratospheric water vapour after 2001: Links to changes in the tropical tropopause and the Brewer-Dobson circulation, J. Geophys. Res., 111, 12312, doi:10.1029/2005JD006744, 2006.

Randel, W. J., Garcia, R., and Wu, F.: Dynamical Balances and Tropical Stratospheric Upwelling, J. Atmos. Sci., 65, 3584, doi:10.1175/2008JAS2756.1, 2008.

Read, W. G., Lambert, A., Bacmeister, J., Cofield, R. E., Christensen, L. E., Cuddy, D. T., Daffer, W. H., Drouin, B. J., Fet-

zer, E., Froidevaux, L., Fuller, R., Herman, R., Jarnot, R. F., Jiang, J. H., Jiang, Y. B., Kelly, K., Knosp, B. W., Kovalenko, L. J., Livesey, N. J., Liu, H.-C., Manney, G. L., Pickett, H. M., Pumphrey, H. C., Rosenlof, K. H., Sabounchi, X., Santee, M. L., Schwartz, M. J., Snyder, W. V., Stek, P. C., Su, H., Takacs, L. L., Thurstans, R. P., Vömel, H., Wagner, P. A., Waters, J. W., Webster, C. R., Weinstock, E. M., and Wu, D. L.: Aura Microwave Limb Sounder upper tropospheric and lower stratospheric H_2O and relative humidity with respect to ice validation, J. Geophys. Res., 112, D24S35, doi:10.1029/2007JD008752, 2007.

Reed, R. J.: A tentative model of the 26-month oscillation in tropical latitudes, Q. J. Roy. Meteorol. Soc., 90, 441–466, doi:10.1002/qj.49709038607, 1964.

Ribera, P., Peña-Ortiz, C., Garcia-Herrera, R., Gallego, D., Gimeno, L., and Hernández, E.: Detection of the secondary meridional circulation associated with the quasi-biennial oscillation, J. Geophys. Res., 109, D18112, doi:10.1029/2003JD004363, 2004.

Roscoe, H. K.: The Brewer-Dobson circulation in the stratosphere and mesosphere-Is there a trend?, Adv. Space Res., 38, 2446–2451, 2006.

Schoeberl, M. R., Douglass, A. R., Stolarski, R. S., Pawson, S., Strahan, S. E., and Read, W. G.: Comparison of lower stratospheric tropical mean vertical velocities, J. Geophys. Res., 113, 24109, doi:10.1029/2008JD010221, 2008.

Schwartz, M. J., Lambert, A., Manney, G. L., Read, W. G., Livesey, N. J., Froidevaux, L., Ao, C. O., Bernath, P. F., Boone, C. D., Cofield, R. E., Daffer, W. H., Drouin, B. J., Fetzer, E. J., Fuller, R. A., Jarnot, R. F., Jiang, J. H., Jiang, Y. B., Knosp, B. W., Krüger, K., Li, J.-L. F., Mlynczak, M. G., Pawson, S., Russell, J. M., Santee, M. L., Snyder, W. V., Stek, P. C., Thurstans, R. P., Tompkins, A. M., Wagner, P. A., Walker, K. A., Waters, J. W., and Wu, D. L.: Validation of the Aura Microwave Limb Sounder temperature and geopotential height measurements, J. Geophys. Res., 113, D15S11, doi:10.1029/2007JD008783, 2008.

Trepte, C. R., Veiga, R. E., and McCormick, M. P.: The poleward dispersal of Mount Pinatubo volcanic aerosol, J. Geophys. Res., 98, 18563–18573, 1993.

Ueyama, R. and Wallace, J. M.: To What Extent Does High-Latitude Wave Forcing Drive Tropical Upwelling in the Brewer-Dobson Circulation?, J. Atmos. Sci., 67, 1232–1246, doi:10.1175/2009JAS3216.1, 2010.

Volk, C., Elkins, J., Fahey, D., Salawitch, R., Dutton, G., Gilligan, J., Proffitt, M., Loewenstein, M., Podolske, J., Minschwaner, K. and Margitan, J. J. and Chan, K. R.: Quantifying transport between the tropical and mid-latitude lower stratosphere, Science, 21, 1763–1768, 1996.

Yulaeva, E., Holton, J. R., and Wallace, J. M.: On the Cause of the Annual Cycle in Tropical Lower-Stratospheric Temperatures, J. Atmos. Sci., 51, 169–174, doi:10.1175/1520-0469(1994)051<0169:OTCOTA>2.0.CO;2, 1994.